Research Article

Haoliang Sun*#, Xinxin Lian#, Xiaoxue Huang, David Hui, and Guangxin Wang

Effects of substrate properties and sputtering methods on self-formation of Ag particles on the Ag–Mo(Zr) alloy films

https://doi.org/10.1515/ntrev-2020-0077
received September 20, 2020; accepted September 25, 2020

Abstract: This article studies two different sputtering methods for depositing Ag–Mo and Ag–Zr alloy films on single crystal silicon (Si), flexible polyimide (PI) and soda-lime glass substrates. The phase structure and the surface morphology of the Ag–Mo(Zr) alloy films were characterized by XRD, SEM and EDS. The effects of substrate properties and sputtering methods on the self-grown Ag particles on the Ag–Mo(Zr) alloy films were investigated. As the result of the experiment, nanoscale Ag particles were formed on the surface of Ag–Mo(Zr) alloy films. However, the size and the number of self-formed Ag particles on the Ag–Mo(Zr) alloy film on the PI substrate are significantly different from that on the Si substrate and glass substrate. This outcome is closely related to the different thermal stress evolution behaviors of the alloy films on different substrates during annealing.

Keywords: Ag–Mo(Zr) alloy film, substrate, thermal stress

1 Introduction

With the increasingly severe service conditions of microdevices, the requirements for the performance of the thin-film materials have gradually increased, leading to extensive applications such as nonenzyme glucose sensors [1], high-strength and high-conductivity films [2], antibacterial films [3], semiconductor interconnect [4], wear-resistant films [5], packaging film materials [6] and so on. There are many methods to prepare thin films, such as electrical deposition [7], arc evaporation [8], wet-laid and spunlace process [9], arc discharge [10] and son on [11], but these methods are not suitable for preparing low solid solubility alloy films. Magnetron sputtering has become an important method for preparing thin films due to its fast speed and good uniformity [12]. The alloy films with low solid solubility prepared by magnetron sputtering, such as Cu–Mn [13], Ag–Ta [14], Cu–Zr [15] and Cu–Ag–Cr [16], are usually in a metastable state, and their atomic diffusion and stress evolution behavior are easily affected by external fields [17]. In particular, as the thickness of the film decreases to the nanometer scale, the atomic diffusion and migration behaviors of the alloy films under the thermal, electric and stress fields become increasingly prominent [18]. Some researchers have shown that the thermal stability of pure Cu and Ag films can be improved by adding a small amount of Zr [19], Cr [20] and Mo [21] elements with the high melting point. However, when more supersaturated alloy elements are added to the alloy film, the larger distortion energy and stress in the film may aggravate the diffusion of atoms [22]. Mo is almost immiscible with Ag at the room temperature, and we had investigated the effect of the microstructure of supersaturated Ag–Mo alloy films on flexible polyimide (PI) substrates by magnetron sputtering in the previous study [23] and found that numerous Ag particles were spontaneously grown on the surface of the as-deposited alloy films [24]. The analysis shows that the main factors affecting the formation of Ag particles on the alloy films are alloy element content [25], film thickness [26] and annealing temperature [27]. In addition to these factors, the properties of the substrate and the sputtering method also have an important influence on the microstructure of the alloy film [28] and the formation of Ag particles [29]. Due to the different crystal structure, surface

# These authors have contributed equally to this work.

*** Corresponding author: Haoliang Sun,** School of Materials Science and Engineering, Henan University of Science and Technology, Luoyang, 471023, China; Collaborative Innovation Center of Nonferrous Metals Henan Province, Luoyang, 471003, China, e-mail: sunhlwm@163.com
Xinxin Lian, Xiaoxue Huang, Guangxin Wang: School of Materials Science and Engineering, Henan University of Science and Technology, Luoyang, 471023, China
David Hui: Department of Mechanical Engineering, University of New Orleans, New Orleans, LA70148, United States of America

morphology and thermal expansion coefficient of different substrates, the alloy films on different substrates have different evolution behaviors of microstructure and residual stress during annealing [30]. In addition, alloy films prepared by co-sputtering deposition and composite target sputtering may have differences in composition uniformity, microstructure and residual stress [31]. Therefore, the authors applied two different sputtering methods to prepare Ag–Mo and Ag–Zr alloy films on PI, Si and glass substrates. The phase structure and surface morphology of the as-deposited and annealed alloy films were characterized by XRD, SEM and EDS. The effects of substrate properties and sputtering methods on the self-growth of Ag particles on the surface of Ag–Mo(Zr) alloy films were investigated.

2 Materials and methods

Composite target sputtering and co-sputtering were applied to deposit Ag–Mo(Zr) alloy films on flexible PI, single-crystal Si(100) and soda-lime glass substrates by JCP-350 magnetron sputtering machine. Composite target is composed of three pieces of Mo(Zr) (10 mm × 10 mm × 1 mm, purity 99.99%) on the surface of a pure Ag target (∅ 50 mm × 4 mm, purity 99.99%), as shown in Figure 1(a). Figure 1(b) is a schematic diagram of dual-target co-sputtering. Co-sputtering is the simultaneous sputtering of a pure Ag target (∅50 mm × 4 mm, purity 99.99%) and a pure Mo(Zr) target (∅50 mm × 4 mm, purity 99.99%).

The flexible PI with the thickness of 125 μm produced by DuPont company, the single-crystal Si(100) and the ordinary soda-lime glass with the size of 10 mm × 10 mm × 1 mm were used as substrates. The acetone, anhydrous ethanol and deionized water were used to clean the substrates in the ultrasonic cleaning machine for 10 min before deposition and then fixed them on the substrate holders. The sputtering power (80–120 W) was adjusted to ensure that the films prepared by the two sputtering methods have the similar composition. The vacuum of the chamber, working pressure and the flow of argon are 5×10^{-4} Pa, 0.4 Pa and 45 sccm, respectively. The distance between the substrate and the target is 7 cm, and the rotation speed of the substrate table is 30 rpm. Some samples are placed in a tube furnace to anneal under the argon protection, and the annealing temperature was 160–360°C.

The microstructure, morphology and composition of Ag–Mo(Zr) alloy films were characterized by X-ray diffraction (XRD; Bruker-AXS D8 Advance, Shimadzu Limited, Kyoto, Japan) (Cu K-alpha) and field emission scanning electron microscope (FE-SEM, JSM 7800F, JEOL Ltd, Tokyo, Japan) with energy dispersive spectroscopy (EDS).

3 Results and discussion

3.1 XRD patterns of the Ag–Mo films by different sputtering methods

Figure 2(a) shows the XRD patterns of the Ag–Mo alloy films deposited on different substrates by composite target sputtering. It can be seen that the diffraction peak intensity of the Ag–Mo alloy film on the PI substrate is significantly weaker than that on the glass and Si substrates. Obviously, the Mo(110) diffraction peak of the Ag–Mo alloy film on the glass is stronger than that on PI and Si substrates, which indicates that the glass substrate is conducive to the growth of Mo(110) grains. The XRD patterns of the Ag–Mo alloy films deposited on different substrates by co-sputtering are shown in Figure 2(b). Evidently, the Mo(110) diffraction peak of Ag–Mo alloy film on the PI substrate is consistent with those on the glass and Si

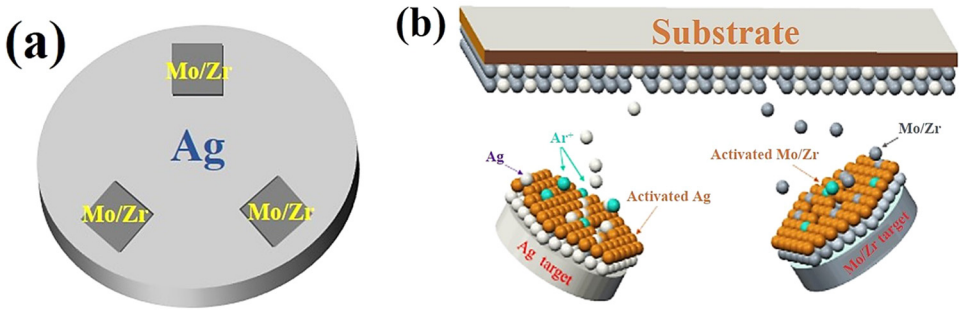

Figure 1: The schematic diagram of sputtering targets: (a) composite target sputtering and (b) co-sputtering.

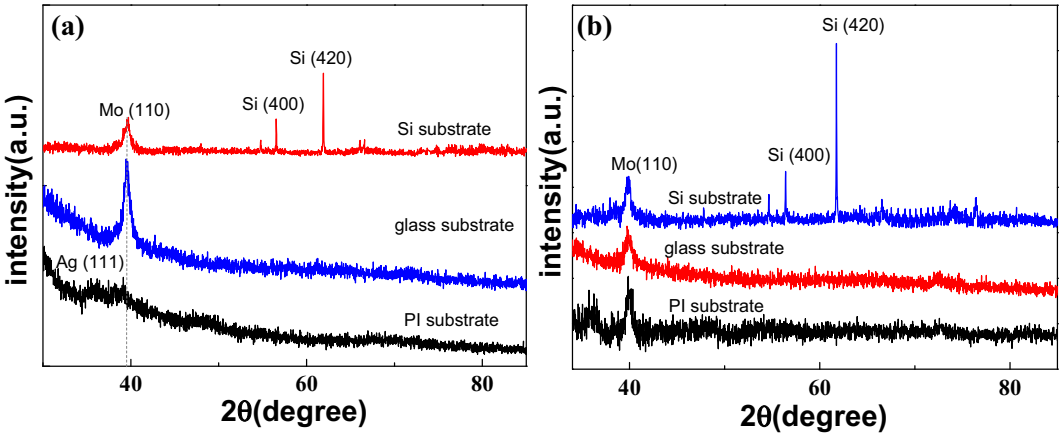

Figure 2: The XRD patterns of Ag–Mo alloy films deposited on different substrates by different sputtering methods: (a) composite target sputtering and (b) co-sputtering.

substrates, which indicates that compared to the alloy films deposited by composite target sputtering, the films prepared on different substrates by co-sputtering have similar microstructure.

3.2 Morphology characterization of the Ag–Mo films on different substrates

Previous studies have found that the Ag content and the film thickness have significant influence on the microstructure of Ag–Mo and Ag–Zr alloy films [32]. In the recent study, it is surprisingly found that the substrate and the sputtering method also have important effects on the formation of Ag particles on the Ag–Mo and Ag–Zr alloy films. Figure 3 shows the SEM images of Ag–Mo alloy films deposited on different substrates by composite target sputtering for 5 min and then annealed at 360°C. It can be seen that many nanoscale polyhedron particles are formed on the Ag–Mo alloy films. In the previous study on the microstructure of Mo–Ag [23,24] and Ag–Zr [19] alloy films, EDS and TEM characterization confirmed that these polyhedral particles are single crystal Ag particles. Ag particles can be fabricated by some different methods, and most of the Ag particles are easy to move and gather, but difficult to fix on the films. The electron beam lithography [33], oxidation–reduction [34] and other methods can fix the Ag particles on the surface of some substrates, but they are complicated and expensive. The authors can self-assemble monodisperse Ag nanoparticles on the surface of the alloy film through a simple method. Moreover, the size and the quantity of these Ag particles are controllable, and they are very firmly bonded to the alloy film. It can be seen from Figure 3(a) that numerous Ag polyhedral particles were grown on the Ag–Mo alloy film/PI substrate. Figure 3(b) is an EDS pattern of the Ag–Mo alloy film/PI substrate, indicating that the contents of Ag and Mo are 50.9% and 49.1%, respectively. Compared with the Ag–Mo alloy film/PI substrate, Figure 3(c and d) shows that the number of polyhedral particles formed on the Ag–Mo alloy film/Si substrate and the Ag–Mo alloy film/glass substrate are much less than that on the Ag–Mo alloy film/PI substrates, which implied that the microstructure and residual stress evolution behavior of the Ag–Mo alloy film/PI substrate are more conducive to the growth of Ag particles.

Figure 3(e), (g) and (h) show the surface morphologies of Ag–Mo alloy films, respectively, deposited on PI, Si and glass substrates by co-sputtering for 5 min and then annealed at 360°C. The morphology of the Ag particles on the three substrates is significantly different from that of the Ag particles prepared by composite target sputtering. Numerous particles are uniformly distributed on the surface of the Ag–Mo film/PI substrate as shown in Figure 3(e), which can be used as surface-enhanced Raman scattering substrates. Moreover, large area particles/films suitable for industrial applications can be easily prepared by using this method, as long as the coating machine and target materials are suitable. The EDS pattern of Figure 3(f) shows that the content of Ag and Mo in the Ag–Mo alloy film is 51.7% and 48.3%, respectively. However, the particle morphologies on the Ag–Mo film/Si substrate and the Ag–Mo film/glass substrate have changed significantly, as shown in Figure 3(g and h). There are many polyhedral particles, and some vermicular particles are grown on the Mo–Ag films/Si substrate, as shown in Figure 3(g). Moreover, it is worth noting that the self-formation Ag particles on the Mo–Ag films/glass substrate

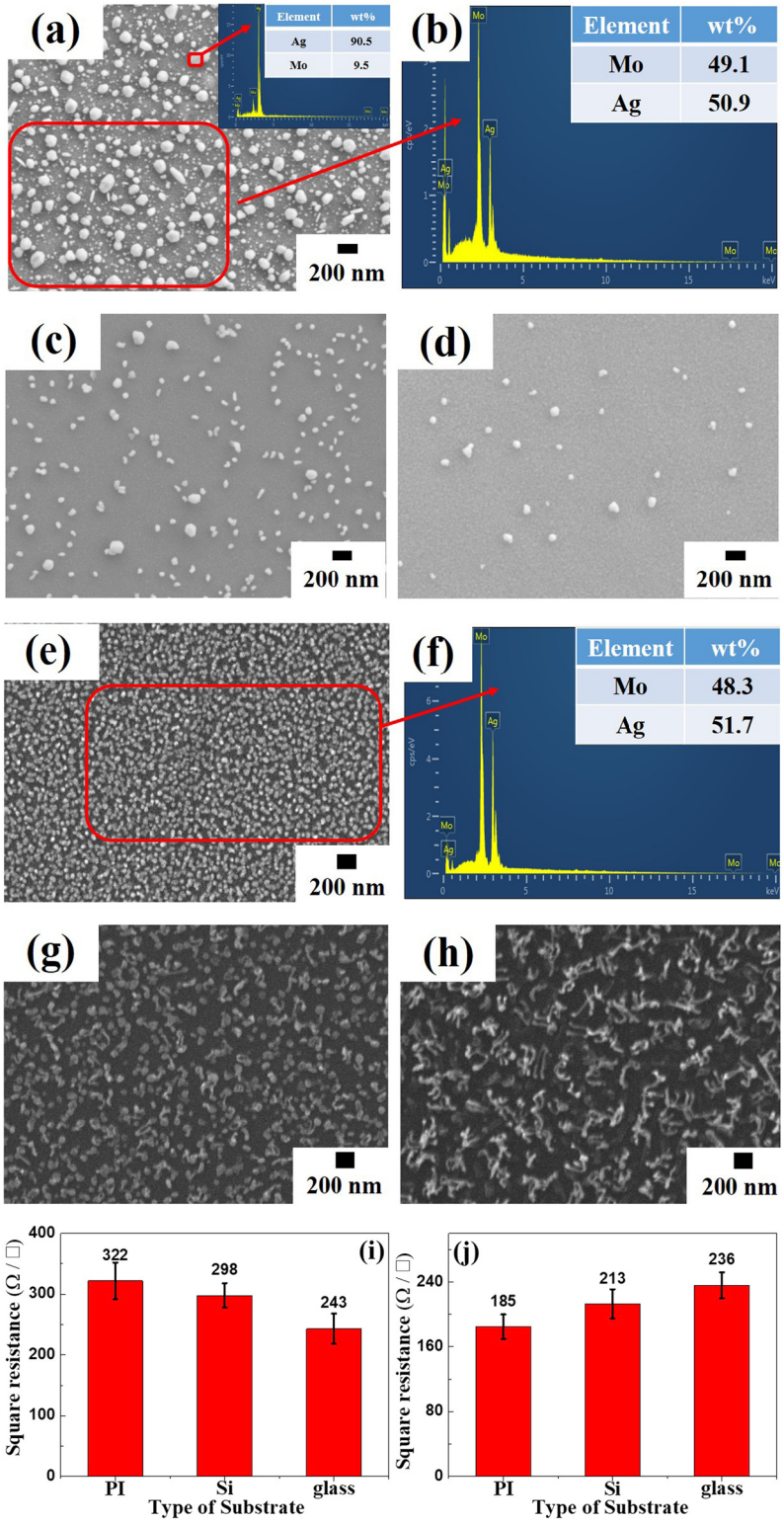

Figure 3: Surface morphology of Ag–Mo alloy films annealed at 360°C on different substrates by composite target sputtering: (a) PI substrate, (b) EDS pattern of (a), (c) Si substrate, (d) glass substrate. surface morphology of the Ag–Mo alloy films annealed at 360°C on different substrates by co-sputtering: (e) PI substrate, (f) EDS pattern of (e), (g) Si substrate, (h) glass substrate; (i) square resistance of Ag–Mo films prepared by composite target sputtering, and (j) square resistance of Ag–Mo films prepared by co-sputtering.

are all vermicular particles as shown in Figure 3(h). The formation mechanism of these vermicular particles is similar to that of Sn whiskers grown on the surface of the Cu–Sn alloy [31]. Its essence is that atoms diffuse along the grain boundary and surface to form Ag particles driven by the release of residual stress and strain energy. At the same time, there are also some defects on the surface of some Ag particles, which leads to the stress gradient inside the particles. Furthermore, some atoms are extruded to form vermicular particles at the defects or edges of the Ag particles driven by the stress gradient. To compare the electrical properties of the Ag–Mo films prepared by different sputtering methods, the authors tested the square resistance of the films through four-point probe resistance. In the case of the Ag–Mo alloy film with the same composition and film thickness, the square resistance of the alloy film mainly depends on the grain size, defects and the uniformity of the alloy film composition in the film. Obviously, comparing Figure 3(i) with Figure 3(j), it is found that the square resistance of the film prepared by co-sputtering is significantly lower than that of the composite target sputtering.

3.3 Surface morphology of the Ag–Zr films on different substrates

The surface morphology of Ag–Zr alloy films on the glass, Si and PI substrates prepared by composite target sputtering after annealing at 260°C is shown in Figure 4(a)–(c). Obviously, some monodisperse polyhedral Ag particles have grown on the surface of the alloy films on the three substrates, and the measurement results show the average size of the Ag particles on the glass, Si and PI substrates were 725, 576, and 156, respectively. The number of self-grown Ag particles on the Ag–Zr film/PI substrates is far more than those on the glass and Si substrates. Moreover, the gap between Ag particles on the Ag–Zr film/PI is much smaller than those on the glass and Si substrates. Figure 4(d)–(f) are the surface morphologies of the annealed Ag–Zr alloy films on different substrates prepared by co-sputtering. Figure 4(f) shows a large number of monodisperse Ag particles uniformly distributed on the Ag–Zr film/PI substrate. The EDS pattern shows that the Ag and Zr content in the alloy film is 85.68% and 14.32%, respectively. Compared with the Ag–Zr film/PI substrate, the number of Ag particles on the Ag–Zr film/glass substrate is significantly reduced, and the size of Ag particles on the Ag–Zr film/Si substrate is significantly decreased. The main reason for this phenomenon is that different types of substrates have different crystal structures, roughness, thermal expansion coefficients and stress release behaviors [35]. These factors directly affect the microstructure, thermal stress and residual stress of the alloy film and further affect the atoms diffusion of the alloy film during annealing.

3.4 Effect of thermal stress on the formation of Ag particles on the Ag–Mo(Zr) film on different substrates

Due to the difference of the thermal expansion coefficients of the three types of substrates and alloy films, large thermal stress will be generated in the alloy films during annealing. We had calculated the thermal stress of Ag–Mo and Ag–Zr thin films generated during annealing by the following formula [36]:

$$\Delta\sigma = \frac{E_{\mathrm{f}}}{(1-\nu_{\mathrm{f}})}\int_{T_1}^{T_2}[\alpha_{\mathrm{f}}(T)-\alpha_{\mathrm{s}}(T)]\,\mathrm{d}T \tag{1}$$

α_{s} and α_f are the thermal expansion coefficients of the substrate and film, respectively. T_1 is the room temperature, T_2 is the annealing temperature. E_{f} is the elastic modulus of the film, ν_{f} is the Poisson's ratio of the film. Elastic modulus and Poisson's ratio of Ag–Mo alloy film are as follows [37]: $E_{\mathrm{f(Ag)}} = 76$ GPa, $E_{\mathrm{f(Mo)}} = 320$ GPa, $E_{\mathrm{f(Ag-Mo)}} = 198$ GPa, $\nu_{f(\mathrm{Ag})} = 0.37$, $\nu_{f(\mathrm{Ag-Mo})} = 0.33$, $\alpha_{\mathrm{Ag}} = 19\times10^{-6}$/K, $\alpha_{\mathrm{Ag-Mo}} = 12.5\times10^{-6}$/K, $\alpha_{\mathrm{glass}} = 7.6\times10^{-6}$/K, $\alpha_{\mathrm{Si}} = 5.2\times10^{-6}$/K and $\alpha_{\mathrm{PI}} = 29.5\times10^{-6}$/K. Calculation based on equation (1) shows that the thermal stress of the Ag–Mo film on three substrates can be estimated as follows: $\Delta\sigma_{\mathrm{glass}} \approx 1.507\times10^6\Delta T$, $\Delta\sigma_{\mathrm{Si}} \approx 2.157\times10^6\Delta T$ and $\Delta\sigma_{\mathrm{PI}} \approx -5.024\times10^6\Delta T$. Due to the low Zr content in the Ag–Zr film, the relevant parameters of the Ag–Zr film adopt the parameters of the Ag film. The thermal stress of the Ag–Zr film on three substrates can be estimated as follows: $\Delta\sigma_{\mathrm{glass}} \approx 1.375\times10^6\Delta T$, $\Delta\sigma_{\mathrm{Si}} \approx 1.665\times10^6\Delta T$, and $\Delta\sigma_{\mathrm{PI}} \approx -1.267\times10^6\Delta T$, as shown in Figure 5.

The thermal expansion coefficient of Si and glass substrates is significantly smaller than that of the Ag–Mo(Zr) alloy film, while the thermal expansion coefficient of PI substrate is significantly larger than that of the Ag–Mo(Zr) alloy film. As a result, the evolution behavior of thermal stress of alloy film on rigid substrates is obviously different from that on flexible substrate [38]. Exactly, the thermal stress of Ag–Mo(Zr) alloy film on the flexible substrate is compressive thermal stress, while that on the rigid substrate is the tensile thermal stress.

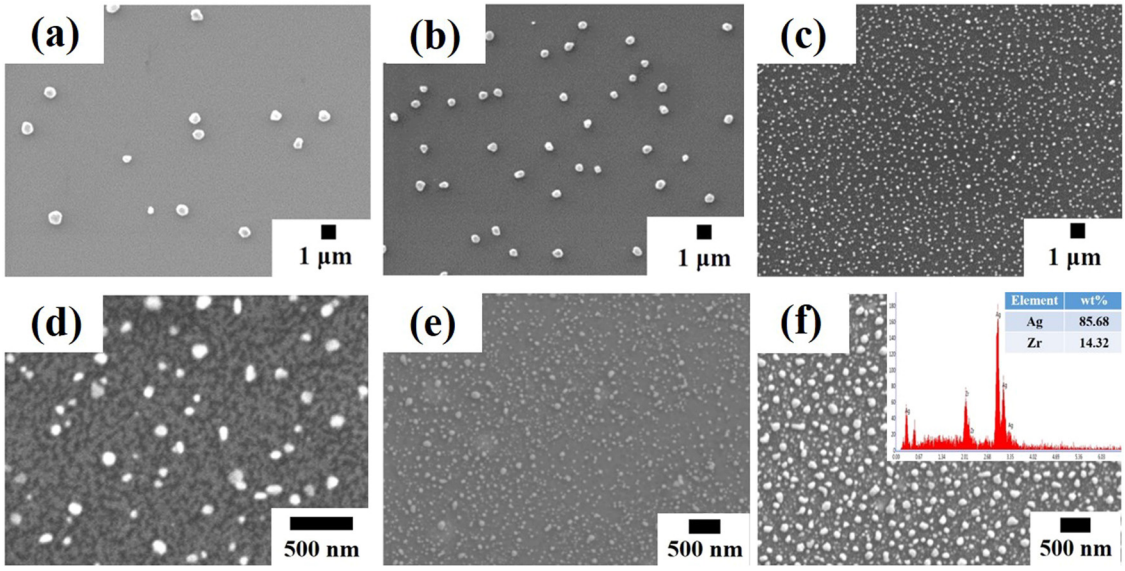

Figure 4: Surface morphology of Ag–Zr alloy films on different substrates by composite target sputtering after annealing at 260°C: (a) glass substrate, (b) Si substrate and (c) PI substrate. Surface morphology of Ag–Zr alloy films on different substrates by co-sputtering: (d) glass substrate, (e) Si substrate and (f) PI substrate.

The release of compressive thermal stress in the film will promote the formation of hillocks or particles on the surface of the alloy film [39], which is the main driven force for the formation of Ag particles on the Ag–Mo(Zr) alloy film on the flexible substrate. However, the tensile stress of the Ag–Mo(Zr) alloy films on the rigid substrate is not conducive to the formation of Ag particles [40]. Based on the aforementioned analysis, it can be concluded that the size and the number of Ag particles formed on the Ag–Mo (Zr) alloy films on different substrates mainly depend on the substrate properties and sputtering methods.

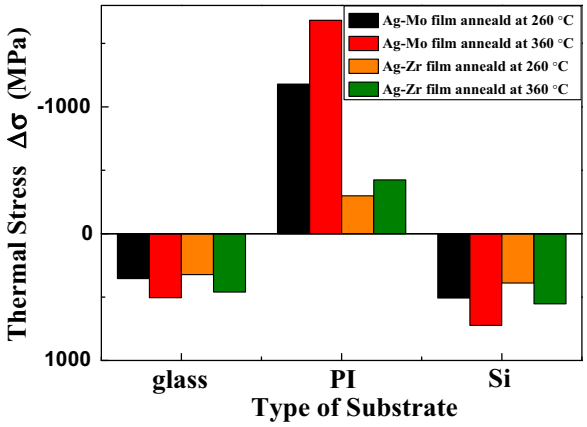

Figure 5: Thermal stress of Ag–Mo and Ag–Zr alloy films on different substrates annealed at 260°C and 360°C.

4 Conclusions

Ag–Mo and Ag–Zr alloy films were fabricated on PI, Si and glass substrates by composite target sputtering and co-sputtering. The results show that a great amount of Ag particles self-grown on the Ag–Mo(Zr) alloy films' surface and the quantity of Ag particles on the PI substrate is significantly more than that on the glass and Si substrates. The reason is that in comparison with the tensile thermal stress in the Ag–Mo(Zr) alloy films bonded on the rigid substrates, the release of compressive thermal stress on the flexible substrate can promote the formation of Ag particles on the alloy films. In addition, the Ag-Mo(Zr) alloy film prepared by co-sputtering has uniform element distribution and fewer defects, which is more conducive to atomic diffusion to form Ag particles.

Acknowledgments: This work was financially supported by the National Natural Science Foundation of China (Grant No. U12041869) and National Undergraduate Entrepreneurship Training Program (Grant number 202010464013).

Conflict of interest: The authors declare no conflict of interest regarding the publication of this paper.

References

[1] Liu SM, Liu BW, Gong CF, Li ZL. A nanoporous Cu–Ag thin film at the Cu–Ag–Zn alloy surface by spontaneous dissolution of Zn and Cu in different degrees as a highly sensitive non-enzymatic glucose sensor. Electrochim Acta. 2019;320:134599.

[2] Zhang XH, Zhang Y, Tian BH, Song KX, Liu P, Jia YL, et al. Review of nano-phase effects in high strength and conductivity copper alloys. Nanotechnol Rev. 2019;8:383–95.

[3] Fu JH, Ji J, Yuan WY, Shen JC. Construction of anti-adhesive and antibacterial multilayer films via layer-by-layer assembly of heparin and chitosan. Biomaterials. 2005;26:6684–92.

[4] Iijima J, Fujii Y, Neishi K, Koike J. Resistivity reduction by external oxidation of Cu Mn alloy films for semiconductor interconnect application. J Vacuum Sci Technol B. 2009;27:1963.

[5] Li JL, Zhang XF, Wang J, Li H, Huang JW, Zhu HG, et al. Mechanical and frictional performance of Ta and Ta–Ag alloy films deposited at different sputtering powers. J Mater Eng Perform. 2019;28:5037–46.

[6] Naseer B, Srivastava G, Qadri OS, Faridi SA, Islam R, Younis K. Importance and health hazards of nanoparticles used in the food industry. Nanotechnol Rev. 2018;7(6):623–41.

[7] Skiba NV. Plastic deformation micromechanism in nanotwinned films. Rev Adv Mater Sci. 2018;57:133–6.

[8] Zhu YJ, Ma JL, Wang GX, Song KX, Heinz RS. Corrosion behaviour of multilayer CrN coatings deposited by hybrid HIPIMS after oxidation treatment. Nanotechnol Rev. 2020;8:596–609.

[9] Zhang GY, Wang D, Xiao Y, Dai JM, Zhang W, Zhang Y. Fabrication of Ag Np-coated wetlace nonwoven fabric based on amino-terminated hyperbranched polymer. Nanotechnol Rev. 2019;8:100–6.

[10] Tseng KH, Chou CJ, Liu TC, Tien DC, Chang CY, Stobinski L. Relationship between Ag nanoparticles and Ag ions prepared by arc discharge method. Nanotechnol Rev. 2018;7:1–9.

[11] Kalwar K, Shen M. Electrospun cellulose acetate nanofibers and Au@AgNPs for antimicrobial activity – a mini review. Nanotechnol Rev. 2019;8:246–57.

[12] Bahce E, Cakir N. Tribological investigation of multilayer CrN/CrCN/TaN films deposited by close field unbalanced magnetron sputtering. Rev Adv Mater Sci. 2019;58:271–9.

[13] Misjak F, Nagy KH, Lobotka P, Radnoczi G. Electron scattering mechanisms in Cu–Mn films for interconnect applications. J Appl Phys. 2014;116:083507.

[14] Zhao M, Liu BX. Formation of an face-centered cubic Ta-rich solid solution by ion beam mixing in the immiscible Ag–Ta system. Metall Mater Trans A. 2010;14:2480–4.

[15] Sun HL, Huang XX, Lian XX, Wang GX. Discrepancies in the microstructures of annealed Cu–Zr bulk alloy and Cu–Zr alloy films. Materials. 2019;12:2467.

[16] Kong LB, Zhou YJ, Song KX, Hui D, Hu H, Guo BJ, et al. Effect of aging on properties and nanoscale precipitates of Cu–Ag–Cr alloy. Nanotechnol Rev. 2020;9:70–8.

[17] Feng J, Liang SH, Guo XH, Zhang Y, Song KX. Electrical conductivity anisotropy of copper matrix composites reinforced with SiC whiskers. Nanotechnol Rev. 2019;8:285–92.

[18] Link S, El-Sayed MA. Spectral properties and relaxation dynamics of surface plasmon electronic oscillations in gold and silver nanodots and nanorods. J Phys Chem B. 1999;103:8410–26.

[19] Huang XX, Sun HL, Wang GX, Stock HR. Self-formation of Ag particles/Ag–Zr alloy films on flexible polyimide as SERS substrates. Appl Surf Sci. 2019;487:1341–7.

[20] Zhang XH, Zhang Y, Tian BH, Jia YL, Liu Y, Song KX, et al. Cr effects on the electrical contact properties of the Al_2O_3–Cu/15W composites. Nanotechnol Rev. 2019;8:128–35.

[21] Chu JP, Lin TN. Deposition, microstructure and properties of sputtered copper films containing insoluble molybdenum. J Appl Phys. 1999;85:6462.

[22] Wang Q, Tu JP, Zhang SC, Lai DM, Peng SM, Gu B. Effect of Ag content on microstructure and tribological performance of WS_2–Ag composite films. Surf Coat Technol. 2006;201:1666–70.

[23] Lian XX, Sun HL, Lv YJ, Wang GX. Room temperature self-assembled Ag nanoparticles/Mo–37.5% Ag film as efficient flexible SERS substrate. Mater Lett. 2020;275:128164.

[24] Lian XX, Lv YJ, Sun HL, Hui D, Wang GX. Effects of Ag contents on the microstructure and SERS performance of self-grown Ag nanoparticles/Mo–Ag alloy films. Nanotechnol Rev. 2020;9:751–9.

[25] Endo Y, Mitsuzuka Y, Shimada Y, Yamaguchi M. Effect of doping elements on the damping constant of $(Ni–Fe)_{1-x}M_x$ (M = Ga, Ag, Mo, and W) films. IEEE Trans Magnet. 2012;48:3390–3.

[26] Wu ZF, Wang XD, Cao QP, Zhao GH, Li JX, Zhang DX, et al. Microstructure characterization of $Al_xCo_1Cr_1Cu_1Fe_1Ni_1$ (x = 0 and 2.5) high-entropy alloy films. J Alloys Compd. 2014;609:137–42.

[27] Sun HL, Huang XX, Lian XX, Wang GX. Adjustment Cu_3Si growth in the interface of annealed Cu–Zr alloy films/Si substrate to form inverted pyramid structure. Mater Lett. 2019;255:126536.

[28] Sun HL, Ma F, Song ZX, Li YH, Xu KW. Effect of substrate constraint on stress-induced deformation mechanism of tungsten thin film. Adv Mater Res. 2010;89–91:539–44.

[29] Ossai CI, Raghavan N. Nanostructure and nanomaterial characterization, growth mechanisms, and applications. Nanotechnol Rev. 2018;7(2):209–31.

[30] Sun HL, Song ZX, Ma F, Xu KW. Stress relaxation induced faceted Cu and W particles on the surfaces of Cu–Zr and W thin films. Appl Surf Sci. 2009;255:8972–7.

[31] Sobiech M, Welzel U, Mittemeijer EJ, Hügel W, Seekamp A. Driving force for Sn whisker growth in the system Cu–Sn. Appl Phys Lett. 2008;93:011906–9.

[32] Sun HL, Lian XX, Lv YJ, Liu YH, Xu C, Dai JW, et al. Effect of annealing on the microstructure and SERS performance of Mo–48.2% Ag films. Materials. 2020;13:4205.

[33] Wang Z, Cai K, Lu Y, Wu HN, Li Y, Zhou QG. Insight into the working wavelength of hotspot effects generated by popular nanostructures. Nanotechnol Rev. 2019;8:24–34.

[34] Adebayo EA, Ibikunle JB, Oke AM, Lateef A, Azeez MA, Oluwatoyin AO, et al. Antimicrobial and antioxidant activity of silver, gold and silver–gold alloy nanoparticles phytosynthesized using extract of *Opuntia ficus*-indica. Rev Adv Mater Sci. 2019;58:313–26.

[35] Tian XX, Xiong SM, Zhang YH, Zhang KP. Simulation of thermal stress in ion beam sputtered Ta_2O_5/SiO_2 multilayer coatings on different substrates by finite element analysis. Surf Coat Technol. 2019;362:225–33.

[36] Zoo Y, Adams D, Mayer JW, Alford TL. Investigation of coefficient of thermal expansion of silver thin film on different substrates using X-ray diffraction. Thin Solid Films. 2006;513:170–4.

[37] Povstenko YZ. Fractional heat conduction eduation and associated thermal stress. J Therm Stress. 2005;28:83102.
[38] Singh CK, Ilango S, Polaki SR, Dash S, Tyag AK. On the evolution of residual stress at different substrate temperatures in sputter-deposited polycrystalline Mo thin films by X-ray diffraction. Mater Res Exp. 2014;1:036401.
[39] Hwang SJ, Nix WD, Joo YC. A model for hillock growth in Al thin films controlled by plastic deformation. Acta Mater. 2007;55:5297–301.
[40] Iwamura E, Ohnishi T, Yoshikawa K. A study of hillock formation on Al–Ta alloy films for interconnections of TFT-LCDs. Thin Solid Films. 1995;270:450–5.